

Type of the Paper (Article)

# 40-Hz auditory steady state response (ASSR) as a biomarker of abnormalities in *SHANK3* gene: a case-report of 15-years old girl with rare microduplication in 22q13.33

Anastasia K Neklyudova<sup>1</sup>, Galina V Portnova<sup>1</sup>, Anna B Rebreikina<sup>1</sup>, Victoria Yu Voinova<sup>2</sup> and Olga V Sysoeva<sup>1\*</sup>

<sup>1</sup> Institute of Higher Nervous Activity and Neurophysiology, Russian Academy of Science, Moscow, Russia; [anastacia.neklyudova@gmail.com](mailto:anastacia.neklyudova@gmail.com), [caviter@list.ru](mailto:caviter@list.ru), [anna.rebreikina@gmail.com](mailto:anna.rebreikina@gmail.com), [olga.v.sysoeva@gmail.com](mailto:olga.v.sysoeva@gmail.com)

<sup>2</sup> Research Clinical Institute of Pediatrics, Moscow Russia; [vivoinova@yandex.ru](mailto:vivoinova@yandex.ru)

\* Correspondence: [olga.v.sysoeva@gmail.com](mailto:olga.v.sysoeva@gmail.com)

**Abstract:** SHANK3 encodes scaffold protein involved in postsynaptic receptor density in glutamatergic synapses, including those in the parvalbumin (PV)+inhibitory neurons – the key players in generation of sensory gamma oscillations, such as 40-Hz auditory steady-state response (ASSR). Here we describe a clinical and neurophysiological phenotype of a 15-years old girl (SH01) with microduplication of 16389 bp in 22q13.33, affecting the SHANK3 gene in comparison to typically developing children (n=32). EEG were recorded during the binaurally presentation of 40-Hz clicks' trains lasting for 500 ms with inter-trial intervals 500-800 ms. SH01 was diagnosed with mild mental retardation and learning disabilities (F70.88) and had problems with reading and writing, as well as smaller vocabulary than TD peers. Her clinical phenotype generally resembled the phenotype of previously described patients with 22q13.33 microduplication. SH01 had mild autistic symptoms but below the threshold for ASD diagnosis. No seizures or MRI abnormalities were reported. While SH01 had relatively preserved auditory event-related potential (ERP) with slightly attenuated P1, her 40-Hz ASSR was totally absent significantly deviating from TD's ASSR. Absence of 40-Hz ASSR in patient with microduplication, affected SHANK3 gene, indicates deficient temporal resolution of the auditory system, that might underlie language problems, and represent neurophysiological biomarker of SHANK3 abnormalities.

**Keywords:** 22q13.3 duplication; Auditory steady state response, ASSR; SHANK3; biomarker; auditory event-related potential, ERP; autism spectrum disorders; intellectual disabilities

## 1. Introduction

SH3 and multiple ankyrin repeat domain 3 (SHANK3), also known as proline-rich synapse-associated protein 2 (ProSAP2), is a gene that encodes scaffolding proteins that organize postsynaptic density in excitatory synapses [1,2]. This gene is in the 22nd chromosome, 22q13.33 region. Deletion of this region as well as mutations lead to 22q13 Deletion Syndrome also known as Phelan-McDermid Syndrome (PMS) [3–6]. In most PMS cases the deletion or mutations affect the SHANK3 gene that is believed to be the major cause of PMS.

Phelan-McDermid Syndrome (PMS) is a rare neurodevelopmental disorder with about 1500 cases identified so far. However, many PMS cases can get unnoticed as the diagnosis of PMS is often difficult due to the subtle appearance of the deletion of chromosome 22 and relatively mild physical and nonspecific clinical manifestation of the syndrome. Dysmorphic features in PMS include dysplastic nails, large or prominent ears, long eyelashes, wide nasal bridge, bulbous nose, and sacral dimple. Major dysfunctions in PMS are hypotonia, global developmental delay, and severely delayed or absent speech. Autistic traits are also present in most patients with PMS, suggesting PMS as a syndromic form of autism spectrum disorder (ASD) [1,7,8]. According to a recent meta-analysis 0.7% of patients with ASD have Shank3 mutations and this number is even higher (2.1%) for ASD patients

with moderate to profound intellectual disability [9]. Moreover, altered methylation patterns in SHANK3 were detected in ~15% of postmortem autistic brain tissue [10], suggesting even more wide-spread implication of altered SHANK3 expression to ASD development through epigenetic influence. Copy-number of variance (CNV) and point mutations of SHANK3 have been also associated with intellectual disability and schizophrenia [9,11–16].

Few cases (n~30) of duplication involving SHANK3 gene has been described in the literature: among patients with Asperger's syndrome, attention-deficit hyperactivity disorder (ADHD), bipolar disorder, schizophrenia, intellectual disabilities, delayed speech and language development [17–21]. Dysmorphic features of patients with duplications, affected SHANK3 gene, included full lips, slightly upturned nose/anteverted nares, protruding ears, arch-shaped eyebrows. Microcephaly was reported in ~15% of reported cases [21]. Each patient had some form of mental problem, however, ASD prevalence seems to be smaller in SHANK3 duplication than in SHANK3 deletions or mutations (~15% vs. >50%). Resemblances between the cases with SHANK3 duplication noticed by the researchers points to a distinct 22q13.33 duplication syndrome (for a recent update see [21,22]). At the same time, implication of both SHANK3 deletion and duplication in neurodevelopmental and neuropsychiatric disorders suggest that SHANK3 gene dosage is essential for correct brain function. However, one must be aware that microduplications does not always mean overexpression of the coded proteins as insertion of genetic material within the gene can alter nucleotide sequence and lead to abnormal protein code. Thus, detailed molecular-genetic analysis is needed to infer about whether the microduplication lead to gain or loss of SHANK3 functioning.

Several animal models of ASD with deficient *Shank3* gene were developed. Mice with *Shank3* mutations/deletion exhibit ASD-like symptoms including social abnormalities and motor coordination problems [10,12,14, 23–30]. The transgenic mice with mildly overexpress *Shank3* proteins (~50%) were also created [18,31,32]. These mice display manic-like hyperkinetic behaviors and decreased social interaction, however, unlike *Shank3* knockout mice (KO), *Shank3* transgenic mice did not exhibit repetitive behavior.

*Shank3* determines the postsynaptic density of N-methyl-D-aspartate (NMDA) receptors. NMDAR is one of three ionotropic receptors to the main excitatory mediator in the brain - glutamate. Deviation in NMDAR function alters excitation/inhibition balance in neuronal circuitry and associates with autistic-like behavior in patients with ASD as well as in its animal models [24]. Noteworthy, different *Shank3* mouse lines show similar NMDAR hypofunction [12, 14, 23–29].

Recent studies pointed to abnormalities in inhibitory signaling in SHANK3-mouse models of ASD. In particular, reduced number of synaptic puncta containing parvalbumin (PV) as well as reduced PV expression of the PV-expressing GABA interneuron, the most abundant subtype of GABAergic interneurons that contributes to perisomatic inhibition of glutamatergic principal cells, were reported [33,14]. Supporting implication of reduced inhibition to SHANK3 deficits, an enhancer of GABA-mediated inhibitory transmission, clonazepam, normalize the abnormal network firing pattern in cultured cortical neurons of *Shank3* KO mice [34].

Cortical gamma oscillations (30-100 Hz) are generated in recurrent circuits of excitatory and inhibitory neurons [35–37] and their amplitude reflects the excitatory state of the neural network. While baseline, spontaneous gamma oscillations are studied in humans and animals, high-frequency oscillations are most reliably induced in response to sensory stimuli [38]. In addition, evoked gamma-band activity can be studied with auditory steady-state response (ASSR) [39–41]. ASSR refers to the ability of the neural populations to synchronize timing of neural discharges with the frequency of external periodic auditory stimulation, e.g. click's trains or amplitude modulated tone. ASSR is most pronounced in response to 40 Hz stimulation [42], coinciding with an intrinsic resonance frequency of cortical PV+ fast-spiking interneurons [43,44]. This 40-Hz ASSR was recently proposed as a non-invasive biomarker of NMDA receptor function [45–48]. The pharmacological modulation of NMDAR function by NMDA antagonists such as MK-801 or ketamine in mice suggested an inverse relationship between ASSR and NMDA occupancy [46, 49]. Nakao and colleagues [45] demonstrated robust ASSR deficits in the mutant mice with selective elimination of NMDARs from PV+ interneurons in neocortex (*Ppp1r2-cre/fGluN1KO*mice) suggesting a causal role of the NMDA

receptors on this PV+ interneurons for neural entrainment at 40 Hz. Modeling studies supported this finding, emphasizing the link between NMDAR on PV+ interneurons and 40-Hz ASSR [50,51].

ASSR is reduced in schizophrenia (for meta-analysis see [52]), bipolar disorders [53–56] and autism spectrum disorders (ASD) [57,58], the disorders with implicated GABAergic dysfunctions and altered NMDA signaling. The 40-Hz ASSR deficit occurs in non-psychotic first-degree relatives of patients with schizophrenia [59] and ASD [57], consistent with an effect of familial or genetic risk factors. However, recent larger sample studies in children with ASD did not confirm ASSR reduction [60,61]. Such discrepancy might be related to the well-known heterogeneity of the ASD population. Even remarkably similar behavioral manifestations can be caused by different biological underpinnings, e.g. genetic etiology. Thus, examination of ASSR for the patient with known genetic abnormalities, associated with ASD, might be Rosetta stone for identification of subgroups of ASD patients based on common molecular-genetic and neurophysiological causes.

Gamma oscillations have been associated with perceptual organization, attention, memory, consciousness, language processing, and motor coordination [62]. The 40-Hz ASSR has been suggested as a candidate mechanism underlying the fast temporal integration and resolution of auditory inputs [39,40,63,64]. In neurotypical controls and elderly population, ASSR was correlated with gap detection threshold [64] and attenuation of speech perception under the presence of noise [63], pointing to the relevance of ASSR to language processing. In patients with schizophrenia the 40-Hz ASSR positively correlated with the working memory performance [65], attentional functioning [66] and predicted the future global symptomatic outcome (GAF-S2) [67]. Thus, ASSR is important for cognitive functioning, altered in patients with SHANK3 abnormalities.

The promising approach in building the causal link between genes and behavior is relating the genetic pathways converging on candidate cellular/molecular processes to the target neurophysiological phenotype. In line with this approach here we present the clinical and neurophysiological description of a 15-years old girl with rare microduplication in 22q13.33, that affects SHANK3 gene. The study focused on examination of 40-Hz ASSR response, that is crucially dependent on PV+interneurons activity, one of key targets of SHANK3 gene. At the behavioral level, ASSR is thought to reflect temporal integration and resolution of auditory system and was linked to memory and speech-in-noise processing. Based on this logic, we hypothesize that this girl will have altered ASSR.

## 2. Results

### 2.1. Genetic information

Our proband, further referred as SH01, has karyotype 46, XX. High resolution molecular karyotyping (SNP Array) results –arr [CRCh37] 22q13.33(51103691\_51120080)x3. Duplication of 16389 bp, affecting the *SHANK3* gene was detected.

### 2.2. Phenotyping, clinical description

SH01 took part in our EEG/ERP experiment at age 15.06 years old. Her official diagnoses were (F70.88) mild mental retardation and other deficits of behavior due to other specified causes, dysgraphia, dyslexia, and (F06.69) organic emotionally labile [asthenic] disorder with unspecified cause. Parents complained of learning disabilities, behavioral disorders, irritability. The girl was sociable but had mild cognitive impairment and mild speech underdevelopment, including rare problems to pronounce long and complex words and smaller vocabulary than TD peers. She used her right hand to write and to eat. Menstruation was regular and has started at 10 years of age. SH01 needed extra support in school but attended normal school together with typically developing peers (TD). She liked to perform in school theatre. At examination she showed infantile behavior, was too dependent on her mom.

Family history and early childhood period. SH01 was from 5th full-term pregnancy from healthy parents, who were 39 years old at the time of the girl's birth. SH01 has an older healthy sister of 30 years (1st pregnancy) and an older brother of 28 years (2nd pregnancy) who has bronchial asthma.

3rd and 4th pregnancies ended in medical abortion. Her weight was 3.040 g and length 52 cm, Apgar score was 7/8. The girl started to hold her head at 2 months, sat down from 6 months, stood with the support at 10 months, began to walk alone from 11 months. The first syllables appeared from 12 months, but there were no phrases for a long time, short sentences appeared from the age of 3. The girl was not interested in books and cartoons until she was 3 years old and then was moderately retarded in mental development. At about this age SH01 developed aggressiveness towards peers and protest behavior that eliminated when she was about 10 years old.

Autistic characteristics. SH01's SRS equals 63 T-scores, which referred to mild autistic symptoms, while neither the Autism Diagnostic Interview-Revised (ADI-R, with subscale social interaction A – 4 scores, Communication and language B – 2, repetitive and restricted behavior C – 1, early developmental problems, 1-36months, D - 1) nor psychiatric assessment suggest ASD.

Intellectual ability. Weckler verbal IQ = 71; nonverbal IQ = 64; full IQ = 64.

Physical parameters at the age of 15: height is 163 cm (50-75 percentile), weight 50 kg (50-75 percentile), head circumference 51.5 cm (lower the 3rd percentile). Facial phenotype included elongated face, protruding auricles. There were short 5th fingers on the hands, a sandal gap. The girl had mild scoliosis, valgus deformity of the knee joints, planovalgus feet.

MRI: The hemispheres of the brain were symmetrical. No focal changes in the intensity of the MR signal from the substance of the brain, cerebellum, or brain stem were found. Differentiation into cortical and medullary substances was expressed satisfactorily. The lateral ventricles are symmetrical, not dilated. The hind horns were deepened. The cerebellum is typically located. The pituitary gland is not changed. Its structure is not broken. The adeno- and neurohypophysis is clearly differentiated. Chiasma has not changed. The optic nerves are clearly visible. The median structures were not displaced. The cranio-vertebral junction is not changed.

Other laboratory examinations. Echocardiography revealed ectopic chords and trabeculae in the left ventricular cavity, mitral valve prolapse with 1+ regurgitation, tricuspid valve prolapse with 1.5+ regurgitation. Ultrasound examination showed bilateral nephroptosis. X-ray showed a short fifth finger metacarpal bone of the left hand. Pulmonary examination revealed moderate bronchial asthma, atopic, with polyvalent sensitization.

Medications: SH01 took Phenibut, 250mg three times a day to control behavior and levothyroxine (L-thyroxine) 50 ml to treat her asthma.

### 2.3. Clinical EEG

The voltage of EEG activity was in accordance with the healthy peers' EEG voltage, significant asymmetry of the background EEG was not detected. EEG recordings when the eyes were closed demonstrated normal background EEG with dominate alpha rhythm (Figure 1(a)). In 2018 it had maximal amplitude 107  $\mu$ V and mean amplitude 87  $\mu$ V and frequency 9.1 Hz in the left hemisphere and maximal amplitude 104  $\mu$ V and mean amplitude 69  $\mu$ V and frequency 9.3 Hz in the right hemisphere. In 2018 dominate alpha-rhythm when the eyes were closed had maximal amplitude 93  $\mu$ V and mean amplitude 67  $\mu$ V and frequency 9.5 Hz in the left hemisphere and maximal amplitude 94  $\mu$ V and mean amplitude 63  $\mu$ V and frequency 9.7 Hz in the right hemisphere. The abnormalities of the background EEG (Figure 1(b)) could be described as intermittent theta slowing (3.5 – 5.5 Hz and 80-140  $\mu$ V) in the right hemisphere in 2018; in 2020 abnormalities of the background EEG could be described as sporadic spike and polyspike discharges (100-150  $\mu$ V) arising from the right centrottemporal region.

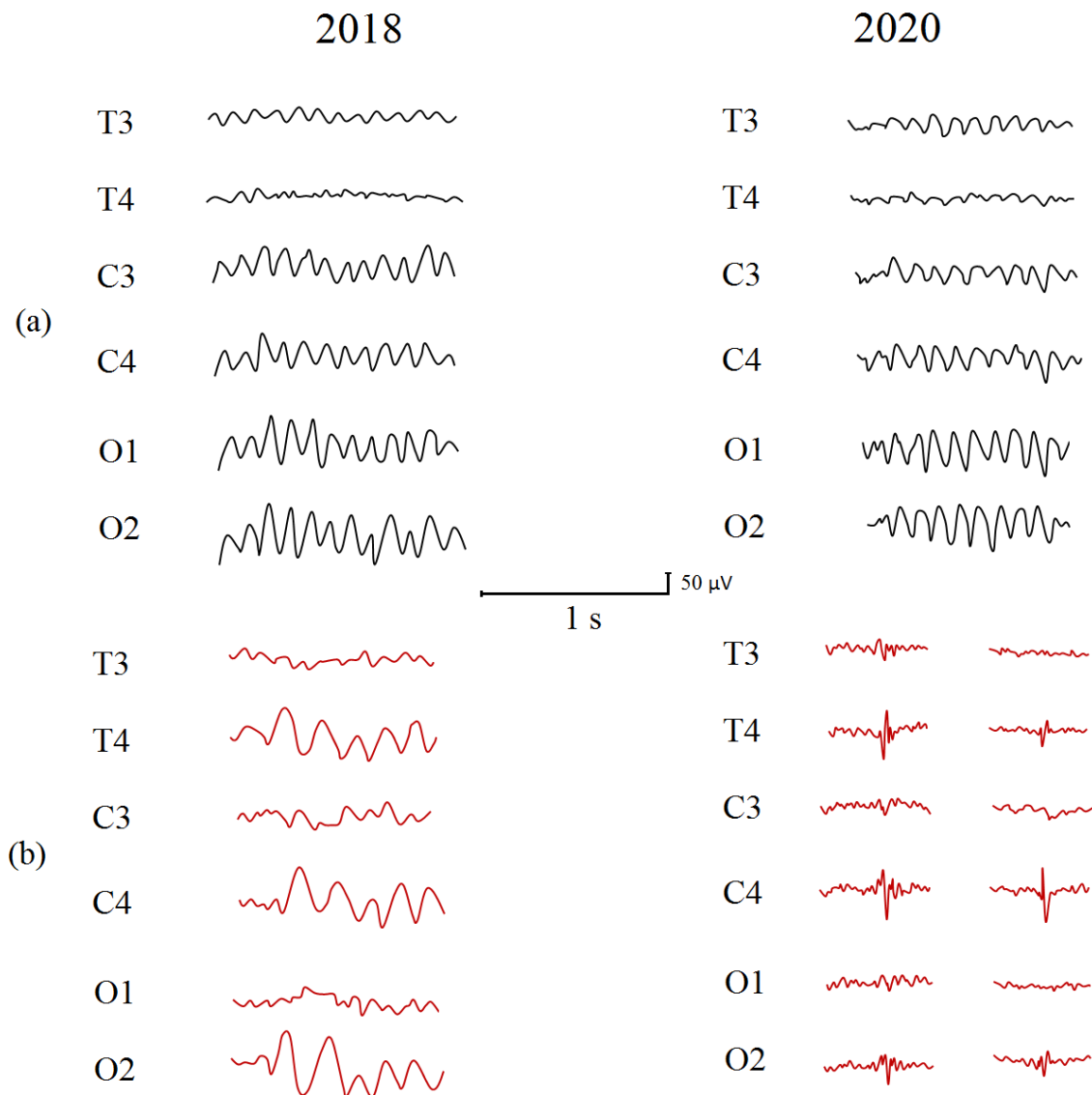


**Figure 1.** (a) - dominate alpha-rhythm when the eyes were closed, (b) - The abnormalities of the background EEG.

#### 2.4. ASSR/AEP

SH01's ASSR and AEP were compared with two control groups of typically developing (TD) children: the first one ('old',  $n=13$ , 7 females, mean age 16.04 (SD = 1.9), ranged 12-18) was age-matched with the participant SH01 (age=15.06). The second sub-group ('young') consisted of 19 participants (14 female, 5 male) with an average age of 7.8 (SD = 2.6), ranged 3-12. Table 1 summarizes the results.

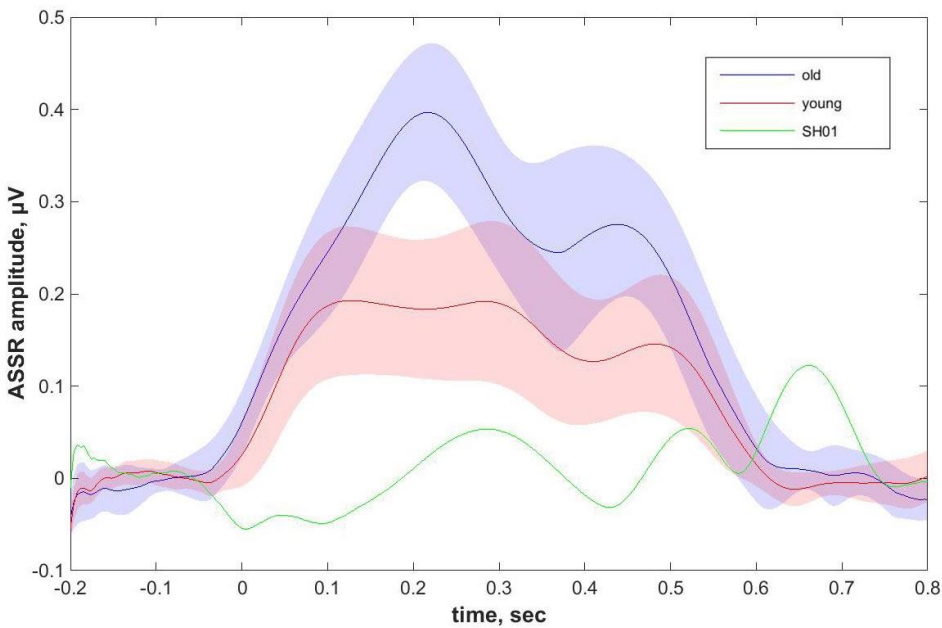
The ASSR was clearly identified in the TD groups and was dominant at frontal sites (Figure 2 and 3). Consistent with previous reports ASSR peaked about 200 ms post-train onset and persisted over the whole period of stimuli presentation in all TD participants, while were significantly higher in the older control group than in the younger one ( $t(30)=2.362$ ,  $p = 0.025$ ), as can be also seen in Figure 4 that represents the individual ASSR values averaged over the whole period of stimuli presentation. At the same time, ASSR were totally absent in SH01 (Figure 2), being significantly smaller compared to any of the groups (old vs SH01:  $t(12)=9.6602$ ,  $p < 0.0001$ ; young vs SH01:  $t(18)=5.684$ ,  $p < 0.0001$ ). Moreover, there were no TD participant in the old, age-matched group who had ASSR value



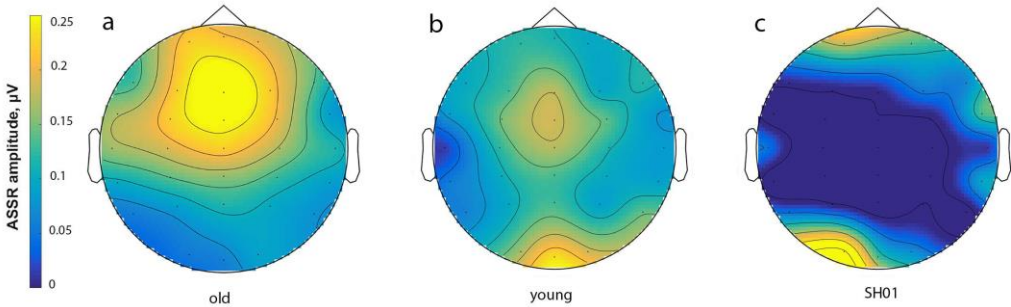
below that of SH01 (minimum value TD old group being 0.053  $\mu$ V, SH01's ASSR = -0.015  $\mu$ V), suggesting very robust effect (Figure 4, Supplementary figure A1).

**Table 1.** Amplitudes of ASSR and ERP components (mean $\pm$ STD) for two comparison groups and SH01 in Fz electrode.

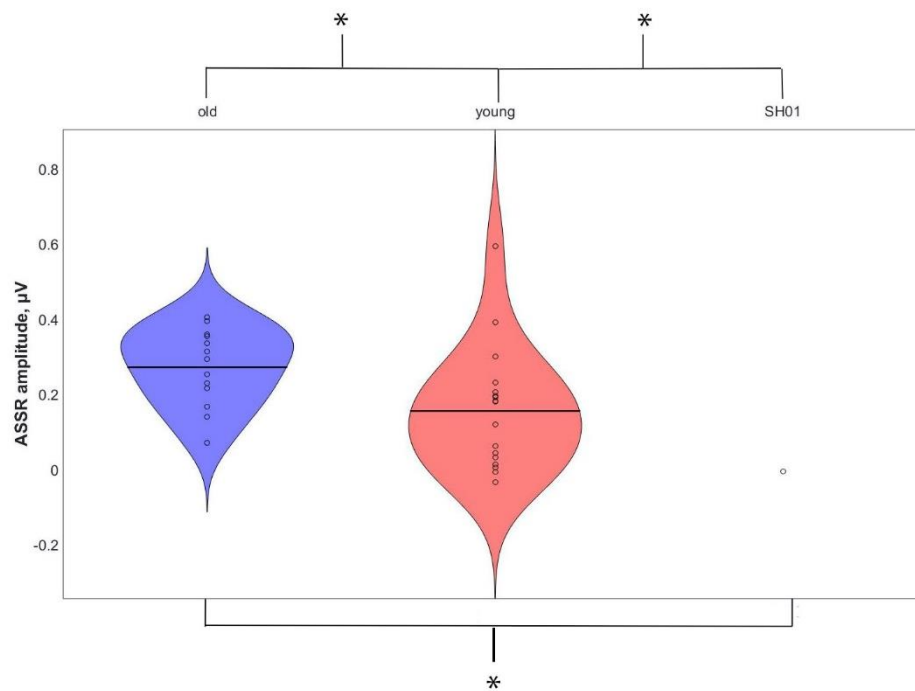
	ASSR, $\mu$ V	P1, $\mu$ V	N1, $\mu$ V	P2, $\mu$ V
SH01 (15.1 y o)	-0.002	1.359	1.102	3.670
Old group (16.1 $\pm$ 1.9 y o)	0.274 $\pm$ 0.103	3.159 $\pm$ 2.017	1.829 $\pm$ 1.885	2.332 $\pm$ 2.241
Young group (7.8 $\pm$ 2.6 y o)	0.158 $\pm$ 0.155	4.267 $\pm$ 1.886	6.059 $\pm$ 3.801	6.455 $\pm$ 4.754



**Figure 2.** Envelope curve of 40-Hz ASSR obtained after Hilbert transform from electrode Fz. The ASSR of SH01 is shown in green, of the younger control group (young) is in red and of the older control group (old) in blue. Opaque blue and red shading illustrate 95% confidence interval. The time of stimulus presentation is 0.

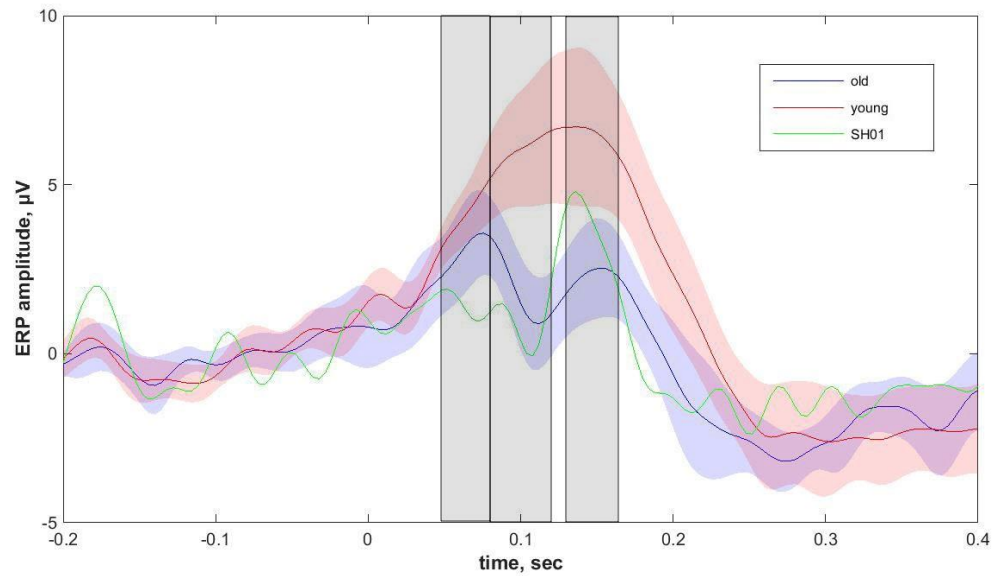


**Figure 3.** Topographic map of ASSR amplitude averaged over the period of 0-500 ms. 'Old' group is represented in Figure 3a, 'young' group is represented in Figure 3b and the values of SH01 is represented in Figure 3c.



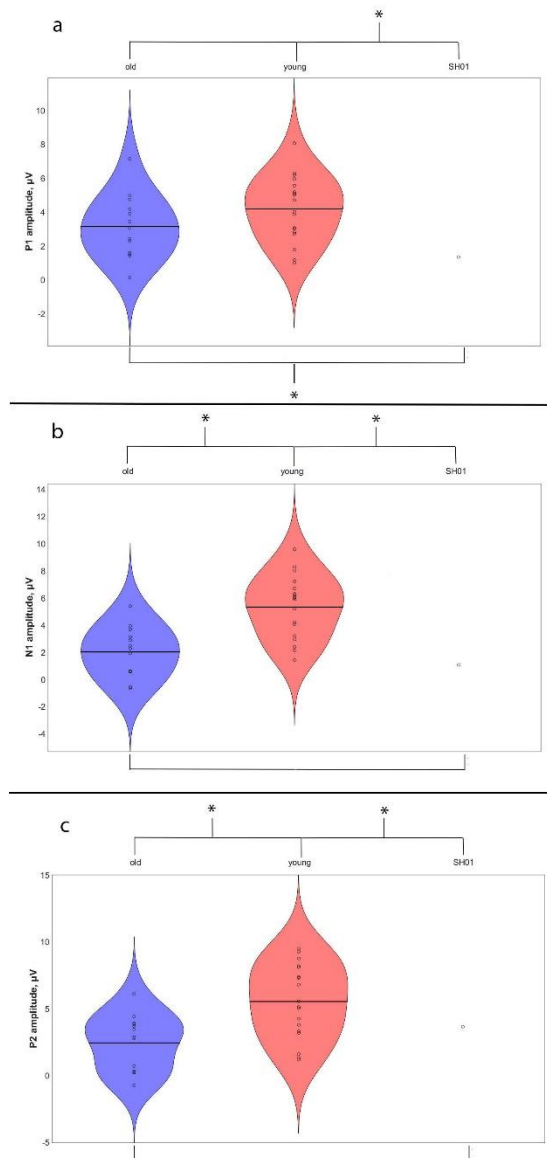
**Figure 4.** Individual values of 40-Hz ASSR across the groups (Fz electrode). Old TD's values are shown in the first column, young TD's values – in a second and SH01's value -- in the third. (\* shows significant differences).

Figure 5 represents the auditory event-related potentials to the same stimuli that fail to elicit ASSR in SH01. Despite such drastic alteration in ASSR response, auditory ERP in SH01 were much more similar to the TD groups (Figure 5, Supplementary Figure A2 for individual ERPs). Old TD group is characterized by prominent P1, N1 and N2 components, registered after train onset. SH01's ERP generally resembles that of old TD ERPs, with only SH01's P1 components being significantly smaller than in her age-matched group ( $t(12)=3.484$ ,  $p = 0.005$ ), while N1 ( $t(12)=1.864$ ,  $p = 0.087$ ) and P2 ( $t(12)=-2.099$ ,  $p = 0.058$ ) being unremarkable as represented in Figure 6. For the peak values of major ERP components see Table 1. As for younger TD participants – their ERPs characterized by the absence of clear N1 response, corresponding with well-known developmental change in ERPs structure (old TD vs. young TD:  $t(30)=-3.524$ ,  $p = 0.0014$ , two-tailed t-test). For all components SH01's ERPs differed from the young groups (P1:  $t(18)=5.683$ ,  $p < 0.0001$ ; N1:  $t(18)=5.863$ ,  $p < 0.0001$ ; P2:  $t(18)=2.554$ ,  $p = 0.02$ ). Thus, auditory ERP in SH01 are closer to her peers than to the young control group.



**Figure 5.** Auditory event-related potentials in Fz electrode with SH01 shown in green, the younger control group (young) in red and the older, age-matched with SH01 control group (old) in blue. Opaque blue and red shading illustrate 95% confidence interval. The time of stimulus presentation is 0. Time windows for P1 (50-80 ms), N1 (80-120 ms) and P2 (130-160 ms) are shown in grey areas.





**Figure 6.** ERPs components across groups. P1 component is shown in Figure 6a, N1 -- in Figure 6b, P2 -- in Figure 6c. Old TD's values are shown in the first column, young TD's values -- in a second and SH01's value -- in the third. (\*) shows significant differences)

### 3. Discussion

Our report presents a new patient with microduplication in 22q13.3 affecting SHANK3 gene, adding one more case to the about 30 patients with 22q13.3 duplications described in previous studies [21]. For the first time we describe neurophysiological phenotype of patient with such microduplication. Major focus of our study was on the 40-Hz ASSR, brain response to high-frequency auditory stimulation, thought to underlie temporal binding and speech-in-noise processing [63]. This choice was motivated by the studies reported 40-Hz ASSR as a biomarker of NMDAR density and PV+ interneurons functioning, as they are dependent on SHANK3 gene activity [46-49]. Here we report a striking absence of 40-Hz ASSR in SH01, collaborating our initial hypothesis. Below we discuss our findings in more details.

Clinical phenotype of SH01 resembles that described for few patients with 22q13.3 microduplication (n=29, [21]). Among common features are intellectual disabilities (n=15), attention deficits (n=4) and language problems (n=5). Physical dysmorphic features have been also reported in these patients previously, including sandal gap (n=1) and protruding or low-set deformed ears (n=3), microcephaly (n=5). One previously described patient with 22q13.3 microduplication [19] shared

with our patient irritability and scoliosis, as well as mild mental retardation and attention deficits. Noteworthy, that girl showed normal development until 13 years old, but later was diagnosed with borderline intellectual functioning and disorganized schizophrenia. At the same time, unlike few patients with 22q13.3 microduplication who were diagnosed with Autism Spectrum Disorders (n=5) and epilepsy (n=4), SH01 do not have epilepsy, only some minor epileptiform activity in EEG, and do not have enough symptoms to get diagnosis of autism spectrum disorder, while her SRS score suggested some autistic features. SH01 shares with 22q13.3 deletion syndrome intellectual disabilities and language problems, as well as autistic features, although their manifestations are milder in SH01 [3,68–70]. Among dysmorphic features reported in patients with PMS SH01 also has elongated skull. Thus, clinical description of SH01 contains both common and distinct features with patients with different types of abnormalities affecting SHANK3, while it more resembles those with SHANK3 microduplications, pointing to partially distinct phenotype of 22q13.3 duplication and deletion.

Our study indicates general preservation of auditory ERP in SH01 with the pronounced N1-P2 response, typical for TD teens. At the same time, P1 component, that usually decreases with age [71,72] is not evident in SH01, with amplitude within P1 latency being significantly smaller in SH01 as compared to the age-matched control group. Unfortunately, we are not aware of any ERP study conducted in patients 22q13.3 microduplication. Thus, we compare our results with those obtained in patients with point mutations or deletion in 22q13.3. Consistent with our finding of reduced P1 response to auditory stimuli, Reese and colleagues [73] found reduction of P50 in response to the repeated tone in patients with PMS. Noteworthy, the reduction was significant only for the female participants. Thus, there might be some common deficits in the early stage of auditory processing in the auditory cortex in patients with abnormalities related to SHANK3 gene. The decrease in the early component of visual ERP to checkerboard stimuli, registered within the same latency range, 50-75 ms post-stimulus were also reported in PMS [74,75], pointing to the fact that neurophysiological abnormalities occurs in PMS at the early stages of sensory processing regardless of the modality of stimulation. We should also point out that attenuation of P1 in response to auditory stimuli was also reported in patients with idiopathic autism [76–78], linking these behavioral and neurophysiological abnormalities.

As for the later components, patients with PMS showed reduction of P2 component in response to the repeated tones [79,73] as well as decrease in the latency of N250 in response to oddball stimuli [80]. In our study, neither P2 nor N250 were affected and P2 even tended to be larger in SH01 than in the age-matched controls. Such discrepancy might indicate different neurophysiological phenotypes for 22q13.3 duplication/deletion or just be related to a methodological difference between the studies.

The focus of our study was ASSR, as we hypothesize its abnormality in our patient based on previous literature. Indeed, we found a striking absence of 40-Hz ASSR in SH01. Considering relatively normal auditory ERP in SH01, such finding points to specific deficits in following high-frequency auditory signal. Absence of 40-Hz ASSR might underlie disruption of temporal integration and binding mechanism in audition, linked with PV+ interneurons functioning. As 40-Hz ASSR was correlated with speech-in-noise perception, absence of ASSR might be related to speech decoding. At the same time, 40-Hz ASSR seems to reflect not a primary mechanism for speech comprehension as the total absence of 40-Hz ASSR does not prevent SH01 from learning language and being fluent in everyday life. Rather 40-Hz ASSR reflects some modulatory mechanism that helps to differentiate speech sounds making it easier to learn and communicate. Abnormalities in such modulatory mechanism can cause low vocabulary and some complex words pronunciation problems, observed in SH01. Further studies are needed to fully examine SH01's phonematic abilities, related to speech perception, to shed light on the particular process disrupted with the absence of 40 Hz ASSR related to SHANK3 abnormality.

While ASSR is modulated by age [42,81,82], our 15-years old patient's ASSR was significantly smaller than those obtained in children aged 3-12 years old. Thus, her dysfunction is hard to explain by the developmental delay or such delay should be very profound with SH01's ASSR corresponding to that from TD children under 5-8 years old [83, 84].

While 40-Hz ASSR were previously studied neither in patients with 22q13.3 deletion/duplication nor their animal models, Engineer and colleagues [85] observed drastic attenuation of neuronal firing rate in response to rapid sounds in the *Shank3*-deficient rat model. These authors showed that the number of driven spikes evoked by noise bursts and speech sounds as well as the spontaneous firing rate was significantly weaker in *Shank3*-deficient rats compared to control rats. But the effect was most pronounced when the stimuli were presented with short inter-stimulus intervals below 100 ms especially in the primary auditory cortex and anterior auditory field. Taken together, the results point to the problems of following the rapidly presented auditory signal as general phenomena, related to SHANK3 abnormalities. This might indicate that gain and loss of SHANK3 function share common neurophysiological phenotype. It might also point to the potential disruption effect of microduplication within the *SHANK3* gene. More detailed molecular genetic analysis and modelling might help to resolve these alternatives.

Our study has implication to the heterogeneous population of idiopathic ASD with significant percentage of its cases related to SHANK3 abnormalities and having language problems. ASSR being easy to assess non-invasive index of functioning of PV+ neurons and NMDAR signaling, stemming from SHANK3 abnormalities, can help to segregate ASD population based on neurophysiological and molecular genetic underpinnings.

Our study is not without limitations. First, it is just a case-report of one patient's data. While SH01 is an incredibly unique patient, more studies are needed to confirm our observations. As less than 30 patients described so far, our study aims to promote the ASSR paradigm among other researchers and clinicians inviting them to run ASSR in other patients with 22q13.3 duplication identified world-wide. These studies are an important step towards validation of this neurophysiological biomarker.

SH01 also took Phenibut as regular medicine. As this drug is a GABA-receptor agonist, it might potentially influence ASSR. To rule out such an explanation we compared SH01 with a kid without known genetic abnormalities, who also took Phenibut for migraine treatment. Such control kid exhibits significant ASSR (Appendix B, Figure B1). At the same time, more research on a larger sample is needed to examine the effects of Phenibut on ASSR.

One may also relate absent 40Ha ASSR to the hearing, arousal level or attention problems, as some researchers found ASSR modulation by these factors [42,86,87]. However, normal auditory ERP in response to the same stimuli rule out these explanations, as e.g. N1 component was also shown to be modulated by attention and stimuli subjective intensity [88]. Moreover, P2 component, that was reported to be attenuated in participants with moderate to severe sensorineural hearing loss [89] even tended to be larger in SH01 pointing to increased rather than decreased auditory sensitivity in SH01.

## 4. Materials and Methods

### 4.1. Participants

Thirty-two typically developing (TD) children were recruited from the local community to take part in a study as a comparison group. According to their parents or guardians, they did not have a history of neuropsychiatric conditions and had normal or corrected to normal vision and hearing. Except for one participant (this case is described in Appendix B) none of the participants reported to be taking any medicines. TD participants were divided into two sub-groups by age (Appendix C, Table C1). The first one ('old') was age-matched with the participant SH01 (age=15.06). It consisted of 13 people (7 female, 6 male) with an average age of 16.04 (SD = 1.9). The second sub-group ('young') consisted of 19 participants (14 female, 5 male) with an average age of 7.8 (SD = 2.6).

Almost all participants' guardians filled Russian translation of the Social Responsiveness Scale, second edition (SRS-2) [90], school age version for young group and school age or adult version for 'old' group. Threshold values for any social behavior deficiencies are 58 T-scores for males and 63 T-scores for females. None of the participants from the old group exceeded threshold value (range 16-56, mean=37, SD=13), and only one participant from the young group had greater value (range 11-62,

mean=27, SD=14). Six participants did not have SRS values. More detailed characteristics of comparison samples are presented in Supplementary Table C1.

SH01 patient undergone full clinical assessment at the Research Clinical Institute of Pediatrics by experienced clinicians. In addition, Autism Diagnostic Interview–Revised [91], an investigator-based semi-structured instrument, was administered by a trained interviewer to SH01' mom. It was used to assess autistic traits in SH01. Genetic testing was done commercially with array comparative genomic hybridization (aCGH), Genoscan 3000 for high resolution molecular karyotyping (Genomed, Russia).

The study was approved by the local ethics committee of the Institute of Higher Nervous Activity and Neurophysiology, Russian Academy of Sciences, and was conducted following the ethical principles regarding human experimentation (Helsinki Declaration). All children provided their verbal consent to participate in the study and were informed about their right to withdraw from the study at any time during the testing. Written informed consent was also obtained from a parent/guardian of each child.

#### 4.2 EEG recording

Electroencephalographic data were recorded using the NeuroTravel system with 32-scalp electrodes arranged according to the international 10–10 system. Ear electrodes were used as reference and the grounding electrode was placed centrally. For clinical EEG periods of resting activity were recorded as well as test on closing and opening the eyes.

#### 4.3 Stimuli and paradigm

The ASSR paradigm consisted with 40 Hz click train stimuli which were presented binaurally through foam insert earphones for 500-ms at 80 dB sound pressure level. Inter-trial intervals varied from 500 to 800 ms. Total number of trials was 150 and the duration of the whole paradigm was around three minutes. Stimuli were presented via Presentation software (NeuroBehavioral Systems, Albany, CA). During the experiment participants were sitting in a dimmed room and watching a silent video of their choice.

#### 4.4 Data analysis

EEG analysis was performed using MATLAB (Version 2014b, The MathWorks, Natick, MA), Fieldtrip software, as well as customized scripts. Peak values were compared using two-tailed Student's t-test for independent groups.

##### 4.4.1 ASSR analysis

First, the raw data were segmented into epochs with an interval of 200 ms before the stimulus and 1000 ms after. Then the signal was filtered at a frequency of 35–45 Hz and trials with amplitude within 3 STD of the mean were averaged. The mean number of selected trials was  $97 \pm 34$  for old group and  $80 \pm 17$  for young group. There were 182 good trials for SH01. To better characterize ASSR we extracted the envelope of the signal using the Hilbert transform. The absolute value of this linear integral transformation reflects the envelope of the grand-average waveform (see Figure C1). Baseline correction for the -200–0 ms were applied. These steps were conducted for all participants, including the patient with microduplication affecting Shank3, SH01. For further analysis we chose the Fz electrode, since according to topographic data (see Figure 3), ASSR has a maximum response near Fz. It is also consistent with the literature, which reports that ASSR is most pronounced in this site [92, 93]. Then we averaged values of the envelope curve after Hilbert transform in Fz electrode over the whole period of stimuli presentation (0–500 ms) and compared the results of SH01 with average values of each comparison group.

#### 4.4.2 ERP analysis

Event-related potentials for auditory stimuli were created with filtering band-pass 1-30 Hz using Fieldtrip function for all participants. Averaging epoch was the same as in ASSR analysis: 200 ms before the stimulus 1000 ms after, but for later analysis we focused on the period of -200-400 ms. Only trials with amplitude within 3 STD of the mean were averaged. The mean number of good trials was  $99 \pm 43$  for old group and  $96 \pm 18$  for young group and 69 for SH01. Then we calculated peak values of event-related potentials for all participants. The timeframes for each component was chosen based on grand-averaged peak latencies (P1: 50-80 ms; N1: 80-120 ms; P2: 130-160 ms).

### 5. Conclusions

Our study demonstrates a link between intragenic copy-number variances (CNVs) of SHANK3 and alteration of brain response to high-frequency auditory input – neurophysiological phenotype mediated by cellular and molecular mechanisms, which depends on the genetic abnormality. This approach gives us hope to bridge the gap between results of noninvasive studies in humans and neurophysiological results obtained in animal models of SHANK3 abnormalities and ASD in general. As such, this step will provide an important contribution to translational research. Reported in our manuscript the absence of 40-Hz ASSR in patient with microduplication, affected SHANK3 gene, indicates deficient temporal resolution of the auditory system, that might underlie language problems, and represent neurophysiological biomarker of SHANK3 abnormalities.

**Supplementary Materials:** Supplementary materials can be found at [www.mdpi.com/xxx/s1](http://www.mdpi.com/xxx/s1).

**Author Contributions:** Conceptualization, O.S.; methodology, O.S. and V.Yu.; data collection, A.N., A.R. and V.Yu.; data analysis, A.N., G.P. and O.S.; resources and data curation, O.S. and V.Yu.; writing—original draft preparation, O.S. and A.N.; writing—review and editing, A.N., G.P. V.Yu., A.R. and O.S.; visualization, A.N. All authors have read and agreed to the published version of the manuscript.

**Funding:** This research was funded by the Russia Science Foundation (RSF), grant #20-68-46042

**Acknowledgments:** We thank all the participants of our study and their parents for their support and dedication to science. This work would not be possible without it.

**Conflicts of Interest:** The authors declare no conflict of interest. The funders had no role in the design of the study; in the collection, analyses, or interpretation of data; in the writing of the manuscript, or in the decision to publish the results.

### Abbreviations

ASD	Autism Spectrum Disorders
ASSR	Auditory Steady State Response
ERP	Event-related potential
TD	Typically developing children
PMS	Phelan-McDermid Syndrome

### Appendix A

Individual ASSRs and ERPs



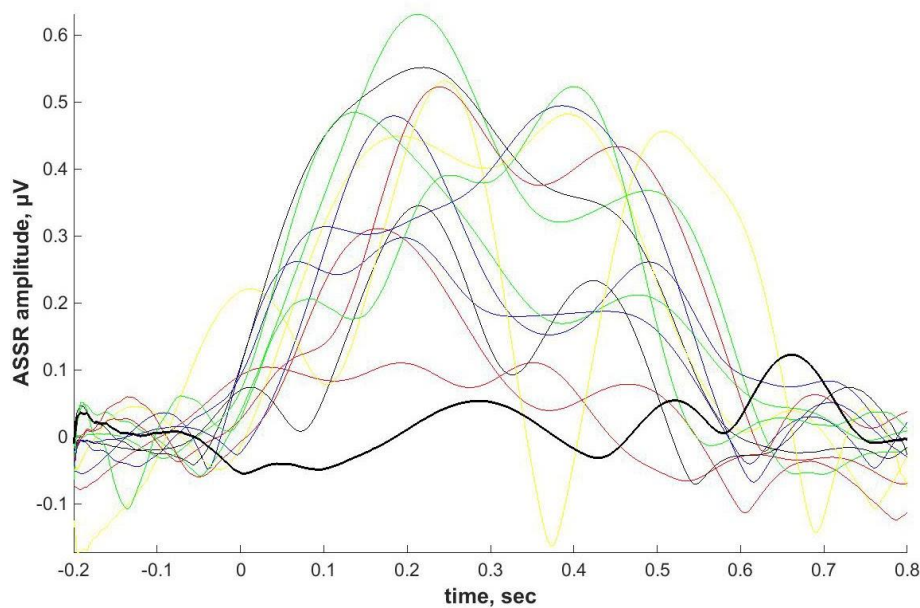


**Figure A1.** Individual values (µV) of 40-Hz ASSR obtained after Hilbert transform for age-matched comparison group ('old') and values of SH01 (presented in bold black). The time of stimulus presentation is 0.

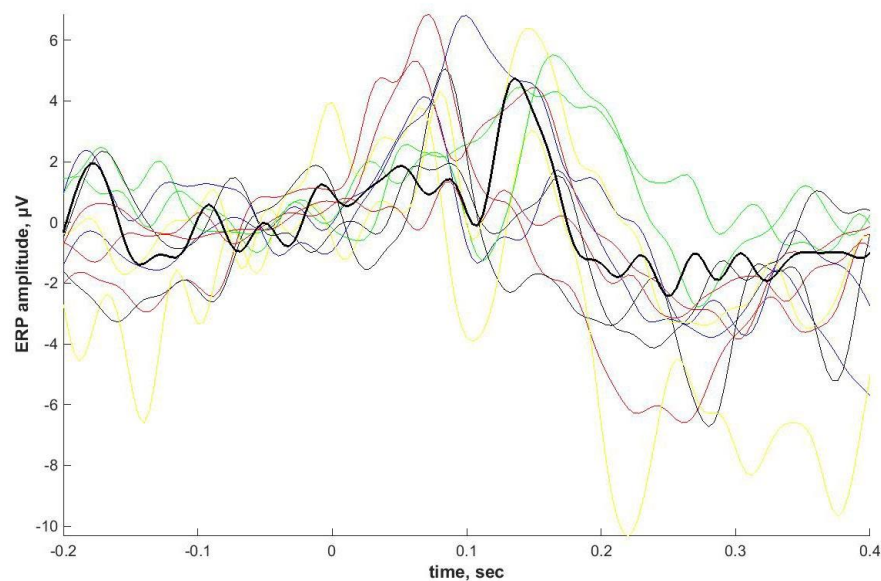


**Figure A2.** Individual ERPs (µV) for age-matched comparison group ('old') and SH01's ERP (presented in bold black).

**Appendix B**

Phenibut effect on ASSR. As mentioned above, one of the participants from young group reported to be taking Phenibut. He was 8.41 years old and had normal SRS T-scores (19). He was taking half a tablet (250 mg) twice a day and was prescribed Phenibut for a migraine attack. As it can be seen in Figure B1, D038 has ASSR within the range of other TD children from the young group



( $t(17)=-0.333$ ,  $p = 0.743$ ) and clearly above that of SH01. Thus, we can conclude that Phenibut does not cause abnormally low ASSR in SH01.

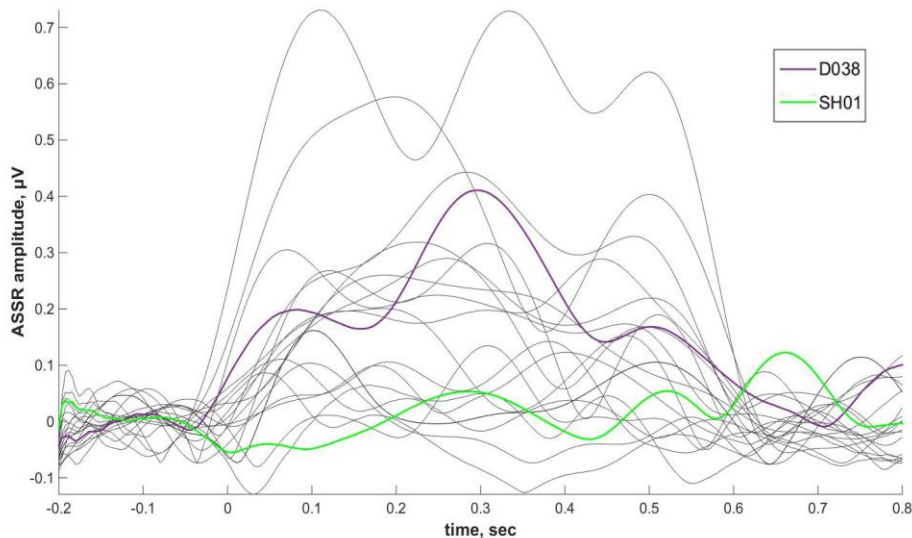


**Figure B1.** Comparison of ASSR values ( $\mu\text{V}$ ) for the participant D038 who took Phenibut (violet) and the participant SH01 (green). Individual amplitudes of ‘young’ group are shown in grey. The time of stimulus presentation is 0.

Appendix C

**Table C1.** Description of comparison groups including age, sex and SRS T-scores.

‘Old’ group				‘Young’ group			
Participant	Age	Sex	SRS, T-scores	Participant	Age	Sex	SRS, T-scores
D015	12.65	f	16	D043	2.58	f	26
D020	12.68	f	39	D033	3.04	m	
D021	13.45	f		D007	5.04	f	
D041	13.94	m	56	D009	5.86	f	22
D002	14.10	f	42	D022	6.01	m	23
D025	14.47	m	24	D012	6.42	f	21
D027	14.76	m	22	D004	7.93	f	15
D047	15.18	m	35	D001	8.18	f	28
D046	15.4	m	52	D006	8.24	f	41
D048	15.74	m	49	D013	8.4	f	22

D049	17, 98	f		D038	8.41	m	19
D050	17.98	f	37	D011	9.04	f	47
D030	17.99	f		D035	9.13	m	62
				D016	9.43	f	11
				D045	9.6	m	12
				D017	9.83	f	
				D014	10.69	f	
				D003	11.98	f	37
				D023	12.04	f	24

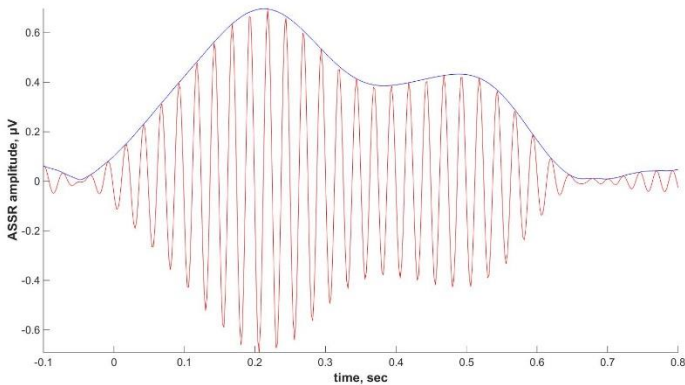


**Figure C1.** Illustration of Hilbert transformation performed for the analysis of ASSR. Red line corresponds with the signal obtain after filtering the data (35-45 Hz) and averaging all good trials. Blue line indicate Hilbert transform of 35-45 Hz filtered ERPs.

References

1. Naisbitt, S.; Kim, E.; Tu, J. C.; Xiao, B.; Sala, C.; Valtschanoff, J.; Weinberg, R. J.; Worley, P. F.; Sheng, M. Shank, a Novel Family of Postsynaptic Density Proteins That Binds to the NMDA Receptor/PSD-95/GKAP Complex and Cortactin. *Neuron* **1999**, 23 (3), 569–582. [https://doi.org/10.1016/s0896-6273\(00\)80809-0](https://doi.org/10.1016/s0896-6273(00)80809-0).

2. Sheng, M.; Kim, E. The Shank Family of Scaffold Proteins. *J Cell Sci* **2000**, 113 ( Pt 11), 1851–1856.

3. Phelan, K.; McDermid, H. E. The 22q13.3 Deletion Syndrome (Phelan-McDermid Syndrome). *Mol Syndromol* **2012**, 2 (3–5), 186–201. <https://doi.org/10.1159/000334260>.

4. Wilson, H. L.; Wong, A. C. C.; Shaw, S. R.; Tse, W.-Y.; Stapleton, G. A.; Phelan, M. C.; Hu, S.; Marshall, J.; McDermid, H. E. Molecular Characterisation of the 22q13 Deletion Syndrome Supports the Role of Haploinsufficiency of SHANK3/PROSAP2 in the Major Neurological Symptoms. *Journal of Medical Genetics* **2003**, 40 (8), 575–584. <https://doi.org/10.1136/jmg.40.8.575>.

5. Costales, J.; Kolevzon, A. Phelan–McDermid Syndrome and SHANK3: Implications for Treatment. *Neurotherapeutics: the journal of the American Society for Experimental NeuroTherapeutics* **2015**, 12. <https://doi.org/10.1007/s13311-015-0352-z>.

6. Harony-Nicolas, H.; De Rubeis, S.; Kolevzon, A.; Buxbaum, J. D. Phelan McDermid Syndrome: From Genetic Discoveries to Animal Models and Treatment. *J Child Neurol* **2015**, 30 (14), 1861–1870. <https://doi.org/10.1177/0883073815600872>.

7. Betancur, C.; Buxbaum, J. D. SHANK3 Haploinsufficiency: A “Common” but Underdiagnosed Highly Penetrant Monogenic Cause of Autism Spectrum Disorders. *Mol Autism* **2013**, *4* (1), 17. <https://doi.org/10.1186/2040-2392-4-17>.
8. Oberman, L. M.; Rotenberg, A.; Pascual-Leone, A. Use of Transcranial Magnetic Stimulation in Autism Spectrum Disorders. *J Autism Dev Disord* **2015**, *45* (2), 524–536. <https://doi.org/10.1007/s10803-013-1960-2>.
9. Leblond, C. S.; Nava, C.; Polge, A.; Gauthier, J.; Huguet, G.; Lumbroso, S.; Giuliano, F.; Stordeur, C.; Depienne, C.; Mouzat, K.; Pinto, D.; Howe, J.; Lemi re, N.; Durand, C. M.; Guibert, J.; Ey, E.; Toro, R.; Peyre, H.; Mathieu, A.; Amsellem, F.; Rastam, M.; Gillberg, I. C.; Rappold, G. A.; Holt, R.; Monaco, A. P.; Maestrini, E.; Galan, P.; Heron, D.; Jacqueline, A.; Afenjar, A.; Rastetter, A.; Brice, A.; Devillard, F.; Assouline, B.; Laffargue, F.; Lespinasse, J.; Chiesa, J.; Rivier, F.; Bonneau, D.; Regnault, B.; Zelenika, D.; Delepine, M.; Lathrop, M.; Sanlaville, D.; Schluth-Bolard, C.; Edery, P.; Perrin, L.; Tabet, A. C.; Schmeisser, M. J.; Boeckers, T. M.; Coleman, M.; Sato, D.; Szatmari, P.; Scherer, S. W.; Rouleau, G. A.; Betancur, C.; Leboyer, M.; Gillberg, C.; Delorme, R.; Bourgeron, T. Meta-Analysis of SHANK Mutations in Autism Spectrum Disorders: A Gradient of Severity in Cognitive Impairments. *PLoS Genet* **2014**, *10* (9), e1004580. <https://doi.org/10.1371/journal.pgen.1004580>.
10. Zhu, L.; Wang, X.; Li, X.-L.; Towers, A.; Cao, X.; Wang, P.; Bowman, R.; Yang, H.; Goldstein, J.; Li, Y.-J.; Jiang, Y.-H. Epigenetic Dysregulation of SHANK3 in Brain Tissues from Individuals with Autism Spectrum Disorders. *Hum Mol Genet* **2014**, *23* (6), 1563–1578. <https://doi.org/10.1093/hmg/ddt547>.
11. Grubruker, A. M.; Schmeisser, M. J.; Schoen, M.; Boeckers, T. M. Postsynaptic ProSAP/Shank Scaffolds in the Cross-Hair of Synaptopathies. *Trends Cell Biol* **2011**, *21* (10), 594–603. <https://doi.org/10.1016/j.tcb.2011.07.003>.
12. Duffney, L. J.; Zhong, P.; Wei, J.; Matas, E.; Cheng, J.; Qin, L.; Ma, K.; Dietz, D. M.; Kajiwar, Y.; Buxbaum, J. D.; Yan, Z. Autism-like Deficits in Shank3-Deficient Mice Are Rescued by Targeting Actin Regulators. *Cell Rep* **2015**, *11* (9), 1400–1413. <https://doi.org/10.1016/j.celrep.2015.04.064>.
13. Alexandrov, P. N.; Zhao, Y.; Jaber, V.; Cong, L.; Lukiw, W. J. Deficits in the Proline-Rich Synapse-Associated Shank3 Protein in Multiple Neuropsychiatric Disorders. *Front Neurol* **2017**, *8*. <https://doi.org/10.3389/fneur.2017.00670>.
14. Monteiro, P.; Feng, G. SHANK Proteins: Roles at the Synapse and in Autism Spectrum Disorder. *Nat Rev Neurosci* **2017**, *18* (3), 147–157. <https://doi.org/10.1038/nrn.2016.183>.
15. Mei, Y.; Monteiro, P.; Zhou, Y.; Kim, J.-A.; Gao, X.; Fu, Z.; Feng, G. Adult Restoration of Shank3 Expression Rescues Selective Autistic-like Phenotypes. *Nature* **2016**, *530* (7591), 481–484. <https://doi.org/10.1038/nature16971>.
16. Sala, C.; Vicidomini, C.; Bigi, I.; Mossa, A.; Verpelli, C. Shank Synaptic Scaffold Proteins: Keys to Understanding the Pathogenesis of Autism and Other Synaptic Disorders. *Journal of Neurochemistry* **2015**, *135* (5), 849–858. <https://doi.org/10.1111/jnc.13232>.
17. Moessner, R.; Marshall, C. R.; Sutcliffe, J. S.; Skaug, J.; Pinto, D.; Vincent, J.; Zwaigenbaum, L.; Fernandez, B.; Roberts, W.; Szatmari, P.; Scherer, S. W. Contribution of SHANK3 Mutations to Autism Spectrum Disorder. *Am J Hum Genet* **2007**, *81* (6), 1289–1297. <https://doi.org/10.1086/522590>.
18. Han, K.; Holder, J. L.; Schaaf, C. P.; Lu, H.; Chen, H.; Kang, H.; Tang, J.; Wu, Z.; Hao, S.; Cheung, S. W.; Yu, P.; Sun, H.; Breman, A. M.; Patel, A.; Lu, H.-C.; Zoghbi, H. Y. SHANK3 Overexpression Causes Manic-like Behaviour with Unique Pharmacogenetic Properties. *Nature* **2013**, *503* (7474), 72–77. <https://doi.org/10.1038/nature12630>.
19. Failla, P.; Romano, C.; Alberti, A.; Vasta, A.; Buono, S.; Castiglia, L.; Luciano, D.; Benedetto, D. D.; Fichera, M.; Galesi, O. Schizophrenia in a Patient with Subtelomeric Duplication of Chromosome 22q. *Clinical Genetics* **2007**, *71* (6), 599–601. <https://doi.org/10.1111/j.1399-0004.2007.00819.x>.
20. Durand, C. M.; Betancur, C.; Boeckers, T. M.; Bockmann, J.; Chaste, P.; Fauchereau, F.; Nygren, G.; Rastam, M.; Gillberg, I. C.; Anckars ter, H.; Sponheim, E.; Goubran-Botros, H.; Delorme, R.; Chabane, N.; Mouren-Simeoni, M.-C.; de Mas, P.; Bieth, E.; Rog , B.; H ron, D.; Burglen, L.; Gillberg, C.; Leboyer, M.; Bourgeron, T. Mutations in the Gene Encoding the Synaptic Scaffolding Protein SHANK3 Are Associated with Autism Spectrum Disorders. *Nat Genet* **2007**, *39* (1), 25–27. <https://doi.org/10.1038/ng1933>.
21. Johannessen, M.; Haugen, I. B.; Bakken, T. L.; Braaten,  . A 22q13.33 Duplication Harbours the SHANK3 Gene: Does It Cause Neuropsychiatric Disorders? *BMJ Case Rep* **2019**, *12* (11). <https://doi.org/10.1136/bcr-2018-228258>.

22. Ujfalusi, A.; Nagy, O.; Bessenyei, B.; Lente, G.; Kántor, I.; Borbély, Á.; Szakszon, K. 22q13 Microduplication Syndrome in Siblings with Mild Clinical Phenotype: Broadening the Clinical and Behavioral Spectrum. *Molecular Syndromology* **2020**, *11*. <https://doi.org/10.1159/000507103>.
23. Kouser, M.; Speed, H. E.; Dewey, C. M.; Reimers, J. M.; Widman, A. J.; Gupta, N.; Liu, S.; Jaramillo, T. C.; Bangash, M.; Xiao, B.; Worley, P. F.; Powell, C. M. Loss of Predominant Shank3 Isoforms Results in Hippocampus-Dependent Impairments in Behavior and Synaptic Transmission. *J Neurosci* **2013**, *33* (47), 18448–18468. <https://doi.org/10.1523/JNEUROSCI.3017-13.2013>.
24. Lee, J.; Chung, C.; Ha, S.; Lee, D.; Kim, D.-Y.; Kim, H.; Kim, E. Shank3-Mutant Mice Lacking Exon 9 Show Altered Excitation/Inhibition Balance, Enhanced Rearing, and Spatial Memory Deficit. *Front. Cell. Neurosci.* **2015**, *9*. <https://doi.org/10.3389/fncel.2015.00094>.
25. Speed, H. E.; Kouser, M.; Xuan, Z.; Reimers, J. M.; Ochoa, C. F.; Gupta, N.; Liu, S.; Powell, C. M. Autism-Associated Insertion Mutation (InsG) of Shank3 Exon 21 Causes Impaired Synaptic Transmission and Behavioral Deficits. *J Neurosci* **2015**, *35* (26), 9648–9665. <https://doi.org/10.1523/JNEUROSCI.3125-14.2015>.
26. Jaramillo, T. C.; Speed, H. E.; Xuan, Z.; Reimers, J. M.; Liu, S.; Powell, C. M. Altered Striatal Synaptic Function and Abnormal Behaviour in Shank3 Exon4-9 Deletion Mouse Model of Autism. *Autism Res* **2016**, *9* (3), 350–375. <https://doi.org/10.1002/aur.1529>.
27. Jiang, Y.-H.; Ehlers, M. D. Modeling Autism by SHANK Gene Mutations in Mice. *Neuron* **2013**, *78* (1), 8–27. <https://doi.org/10.1016/j.neuron.2013.03.016>.
28. Yoo, J.; Bakes, J.; Bradley, C.; Collingridge, G. L.; Kaang, B.-K. Shank Mutant Mice as an Animal Model of Autism. *Philosophical Transactions of the Royal Society B: Biological Sciences* **2014**, *369* (1633). <https://doi.org/10.1098/rstb.2013.0143>.
29. Schmeisser, M. J. Translational Neurobiology in Shank Mutant Mice--Model Systems for Neuropsychiatric Disorders. *Ann Anat* **2015**, *200*, 115–117. <https://doi.org/10.1016/j.aanat.2015.03.006>.
30. Dhamne, S. C.; Silverman, J. L.; Super, C. E.; Lammers, S. H. T.; Hameed, M. Q.; Modi, M. E.; Copping, N. A.; Pride, M. C.; Smith, D. G.; Rotenberg, A.; Crawley, J. N.; Sahin, M. Replicable in Vivo Physiological and Behavioral Phenotypes of the Shank3B Null Mutant Mouse Model of Autism. *Mol Autism* **2017**, *8*. <https://doi.org/10.1186/s13229-017-0142-z>.
31. Choi, S.-Y.; Pang, K.; Kim, J. Y.; Ryu, J. R.; Kang, H.; Liu, Z.; Kim, W.-K.; Sun, W.; Kim, H.; Han, K. Post-Transcriptional Regulation of SHANK3 Expression by MicroRNAs Related to Multiple Neuropsychiatric Disorders. *Mol Brain* **2015**, *8*. <https://doi.org/10.1186/s13041-015-0165-3>.
32. Lee, S.; Lee, E.; Kim, R.; Kim, J.; Lee, S.; Park, H.; Yang, E.; Kim, H.; Kim, E. Shank2 Deletion in Parvalbumin Neurons Leads to Moderate Hyperactivity, Enhanced Self-Grooming and Suppressed Seizure Susceptibility in Mice. *Front Mol Neurosci* **2018**, *11*, 209. <https://doi.org/10.3389/fnmol.2018.00209>.
33. Filice, F.; Vörckel, K. J.; Sungur, A. Ö.; Wöhr, M.; Schwaller, B. Reduction in Parvalbumin Expression Not Loss of the Parvalbumin-Expressing GABA Interneuron Subpopulation in Genetic Parvalbumin and Shank Mouse Models of Autism. *Molecular Brain* **2016**, *9* (1), 10. <https://doi.org/10.1186/s13041-016-0192-8>.
34. Lu, C.; Chen, Q.; Zhou, T.; Bozic, D.; Fu, Z.; Pan, J. Q.; Feng, G. Micro-Electrode Array Recordings Reveal Reductions in Both Excitation and Inhibition in Cultured Cortical Neuron Networks Lacking Shank3. *Mol Psychiatry* **2016**, *21* (2), 159–168. <https://doi.org/10.1038/mp.2015.173>.
35. Bartos, M.; Vida, I.; Jonas, P. Synaptic Mechanisms of Synchronized Gamma Oscillations in Inhibitory Interneuron Networks. *Nat Rev Neurosci* **2007**, *8* (1), 45–56. <https://doi.org/10.1038/nrn2044>.
36. Vinck, M.; Womelsdorf, T.; Buffalo, E. A.; Desimone, R.; Fries, P. Attentional Modulation of Cell-Class-Specific Gamma-Band Synchronization in Awake Monkey Area V4. *Neuron* **2013**, *80* (4), 1077–1089. <https://doi.org/10.1016/j.neuron.2013.08.019>.
37. Carlén, M.; Meletis, K.; Siegle, J. H.; Cardin, J. A.; Futai, K.; Vierling-Claassen, D.; Rühlmann, C.; Jones, S. R.; Deisseroth, K.; Sheng, M.; Moore, C. I.; Tsai, L.-H. A Critical Role for NMDA Receptors in Parvalbumin Interneurons for Gamma Rhythm Induction and Behavior. *Molecular Psychiatry* **2012**, *17* (5), 537–548. <https://doi.org/10.1038/mp.2011.31>.
38. Hoogenboom, N.; Schoffelen, J.-M.; Oostenveld, R.; Parkes, L. M.; Fries, P. Localizing Human Visual Gamma-Band Activity in Frequency, Time and Space. *Neuroimage* **2006**, *29* (3), 764–773. <https://doi.org/10.1016/j.neuroimage.2005.08.043>.
39. Ross, B.; Picton, T.; Pantev, C. Temporal Integration in the Human Auditory Cortex as Represented by the Development of the Steady-State Magnetic Field. *Hearing research* **2002**, *165*, 68–84. [https://doi.org/10.1016/S0378-5955\(02\)00285-X](https://doi.org/10.1016/S0378-5955(02)00285-X).

40. Ross, B.; Pantev, C. Auditory Steady-State Responses Reveal Amplitude Modulation Gap Detection Thresholds. *The Journal of the Acoustical Society of America* **2004**, *115*, 2193–2206. <https://doi.org/10.1121/1.1694996>.
41. Onitsuka, T.; Oribe, N.; Nakamura, I.; Kanba, S. Review of Neurophysiological Findings in Patients with Schizophrenia. *Psychiatry and Clinical Neurosciences* **2013**, *67* (7), 461–470. <https://doi.org/10.1111/pcn.12090>.
42. Picton, T. W.; John, M. S.; Dimitrijevic, A.; Purcell, D. Human Auditory Steady-State Responses. *Int J Audiol* **2003**, *42* (4), 177–219. <https://doi.org/10.3109/14992020309101316>.
43. Tateno, T.; Harsch, A.; Robinson, H. P. C. Threshold Firing Frequency-Current Relationships of Neurons in Rat Somatosensory Cortex: Type 1 and Type 2 Dynamics. *J Neurophysiol* **2004**, *92* (4), 2283–2294. <https://doi.org/10.1152/jn.00109.2004>.
44. Golomb, D.; Donner, K.; Shacham, L.; Shlosberg, D.; Amitai, Y.; Hansel, D. Mechanisms of Firing Patterns in Fast-Spiking Cortical Interneurons. *PLOS Computational Biology* **2007**, *3* (8), e156. <https://doi.org/10.1371/journal.pcbi.0030156>.
45. Nakao, K.; Nakazawa, K. Brain State-Dependent Abnormal LFP Activity in the Auditory Cortex of a Schizophrenia Mouse Model. *Front Neurosci* **2014**, *8*, 168. <https://doi.org/10.3389/fnins.2014.00168>.
46. Sivarao, D. V.; Chen, P.; Senapati, A.; Yang, Y.; Fernandes, A.; Benitez, Y.; Whiterock, V.; Li, Y.-W.; Ahljanian, M. K. 40 Hz Auditory Steady-State Response Is a Pharmacodynamic Biomarker for Cortical NMDA Receptors. *Neuropsychopharmacology* **2016**, *41* (9), 2232–2240. <https://doi.org/10.1038/npp.2016.17>.
47. Sullivan, E. M.; Timi, P.; Hong, L. E.; O'Donnell, P. Effects of NMDA and GABA-A Receptor Antagonism on Auditory Steady-State Synchronization in Awake Behaving Rats. *Int J Neuropsychopharmacol* **2015**, *18* (7). <https://doi.org/10.1093/ijnp/pyu118>.
48. Leishman, E.; O'Donnell, B. F.; Millward, J. B.; Vohs, J. L.; Rass, O.; Krishnan, G. P.; Bolbecker, A. R.; Morzorati, S. L. Phencyclidine Disrupts the Auditory Steady State Response in Rats. *PLoS One* **2015**, *10* (8). <https://doi.org/10.1371/journal.pone.0134979>.
49. Sivarao, D.; Frenkel, M.; Chen, P.; Healy, F.; Lodge, N.; Zaczek, R. MK-801 Disrupts and Nicotine Augments 40 Hz Auditory Steady State Responses in the Auditory Cortex of the Urethane-Anesthetized Rat. *Neuropharmacology* **2013**, *73*. <https://doi.org/10.1016/j.neuropharm.2013.05.006>.
50. Kirli, K. K.; Ermentrout, G. B.; Cho, R. Y. Computational Study of NMDA Conductance and Cortical Oscillations in Schizophrenia. *Front. Comput. Neurosci.* **2014**, *8*. <https://doi.org/10.3389/fncom.2014.00133>.
51. Spencer, K. M. The Functional Consequences of Cortical Circuit Abnormalities on Gamma Oscillations in Schizophrenia: Insights from Computational Modeling. *Front Hum Neurosci* **2009**, *3*. <https://doi.org/10.3389/neuro.09.033.2009>.
52. Thuné, H.; Recasens, M.; Uhlhaas, P. The 40-Hz Auditory Steady-State Response in Patients With Schizophrenia: A Meta-Analysis. *JAMA Psychiatry* **2016**, *73*. <https://doi.org/10.1001/jamapsychiatry.2016.2619>.
53. Parker, D.; Hamm, J.; McDowell, J.; Keedy, S.; Gershon, E.; Ivleva, E.; Pearlson, G.; Keshavan, M.; Tamminga, C.; Sweeney, J.; Clementz, B. Auditory Steady-State EEG Response across the Schizo-Bipolar Spectrum. *Schizophrenia Research* **2019**, *209*. <https://doi.org/10.1016/j.schres.2019.04.014>.
54. Isomura, S.; Onitsuka, T.; Tsuchimoto, R.; Nakamura, I.; Hirano, S.; Oda, Y.; Oribe, N.; Hirano, Y.; Ueno, T.; Kanba, S. Differentiation between Major Depressive Disorder and Bipolar Disorder by Auditory Steady-State Responses. *Journal of Affective Disorders* **2016**, *190*, 800–806. <https://doi.org/10.1016/j.jad.2015.11.034>.
55. Rass, O.; Krishnan, G.; Brenner, C. A.; Hetrick, W. P.; Merrill, C. C.; Shekhar, A.; O'Donnell, B. F. Auditory Steady State Response in Bipolar Disorder: Relation to Clinical State, Cognitive Performance, Medication Status, and Substance Disorders. *Bipolar Disord* **2010**, *12* (8), 793–803. <https://doi.org/10.1111/j.1399-5618.2010.00871.x>.
56. Oda, Y.; Onitsuka, T.; Tsuchimoto, R.; Hirano, S.; Oribe, N.; Ueno, T.; Hirano, Y.; Nakamura, I.; Miura, T.; Kanba, S. Gamma Band Neural Synchronization Deficits for Auditory Steady State Responses in Bipolar Disorder Patients. *PLoS One* **2012**, *7* (7). <https://doi.org/10.1371/journal.pone.0039955>.
57. Rojas, D. C.; Teale, P. D.; Maharajh, K.; Kronberg, E.; Youngpeter, K.; Wilson, L. B.; Wallace, A.; Hepburn, S. Transient and Steady-State Auditory Gamma-Band Responses in First-Degree Relatives of People with Autism Spectrum Disorder. *Molecular Autism* **2011**, *2* (1), 11. <https://doi.org/10.1186/2040-2392-2-11>.



58. Seymour, R. A.; Rippon, G.; Gooding-Williams, G.; Sowman, P. F.; Kessler, K. Reduced Auditory Steady State Responses in Autism Spectrum Disorder. *Molecular Autism* **2020**, *11* (1), 56. <https://doi.org/10.1186/s13229-020-00357-y>.
59. Hong, L. E.; Summerfelt, A.; McMahon, R.; Adami, H.; Francis, G.; Elliott, A.; Buchanan, R. W.; Thaker, G. K. Evoked Gamma Band Synchronization and the Liability for Schizophrenia. *Schizophrenia Research* **2004**, *70* (2), 293–302. <https://doi.org/10.1016/j.schres.2003.12.011>.
60. Ono, Y.; Kudoh, K.; Ikeda, T.; Takahashi, T.; Yoshimura, Y.; Minabe, Y.; Kikuchi, M. Auditory Steady-State Response at 20 Hz and 40 Hz in Young Typically Developing Children and Children with Autism Spectrum Disorder. *Psychiatry and Clinical Neurosciences* **2020**, *74* (6), 354–361. <https://doi.org/10.1111/pcn.12998>.
61. Stroganova, T.; Komarov, K.; Goiaeva, D.; Obukhova, T.; Ovsiannikova, T.; Prokofiev, A.; Orekhova, E. Left Hemispheric Deficit in the Sustained Neuromagnetic Response to Periodic Click Trains in Children with ASD.; 2020. <https://doi.org/10.21203/rs.3.rs-48864/v1>.
62. Uhlhaas, P. J.; Haenschel, C.; Nikolić, D.; Singer, W. The Role of Oscillations and Synchrony in Cortical Networks and Their Putative Relevance for the Pathophysiology of Schizophrenia. *Schizophr Bull* **2008**, *34* (5), 927–943. <https://doi.org/10.1093/schbul/sbn062>.
63. Ross, B.; Fujioka, T. 40-Hz Oscillations Underlying Perceptual Binding in Young and Older Adults: Perceptual Binding and Aging. *Psychophysiology* **2016**, *53*. <https://doi.org/10.1111/psyp.12654>.
64. Baltus, A.; Herrmann, C. Auditory Temporal Resolution Is Linked to Resonance Frequency of the Auditory Cortex. *International journal of psychophysiology: official journal of the International Organization of Psychophysiology* **2015**, *98*. <https://doi.org/10.1016/j.ijpsycho.2015.08.003>.
65. Light, G. A.; Hsu, J. L.; Hsieh, M. H.; Meyer-Gomes, K.; Sprock, J.; Swerdlow, N. R.; Braff, D. L. Gamma Band Oscillations Reveal Neural Network Cortical Coherence Dysfunction in Schizophrenia Patients. *Biol Psychiatry* **2006**, *60* (11), 1231–1240. <https://doi.org/10.1016/j.biopsych.2006.03.055>.
66. Tada, M.; Nagai, T.; Kirihaara, K.; Koike, S.; Suga, M.; Araki, T.; Kobayashi, T.; Kasai, K. Differential Alterations of Auditory Gamma Oscillatory Responses Between Pre-Onset High-Risk Individuals and First-Episode Schizophrenia. *Cereb Cortex* **2016**, *26* (3), 1027–1035. <https://doi.org/10.1093/cercor/bhu278>.
67. Koshiyama, D.; Kirihaara, K.; Tada, M.; Nagai, T.; Fujioka, M.; Ichikawa, E.; Ohta, K.; Tani, M.; Tsuchiya, M.; Kanehara, A.; Morita, K.; Sawada, K.; Matsuoka, J.; Satomura, Y.; Koike, S.; Suga, M.; Araki, T.; Kasai, K. Electrophysiological Evidence for Abnormal Glutamate-GABA Association Following Psychosis Onset. *Transl Psychiatry* **2018**, *8*. <https://doi.org/10.1038/s41398-018-0261-0>.
68. Philippe, A.; Boddaert, N.; Vaivre-Douret, L.; Robel, L.; Danon-Boileau, L.; Malan, V.; de Blois, M.-C.; Heron, D.; Colleaux, L.; Golse, B.; Zilbovicius, M.; Munnich, A. Neurobehavioral Profile and Brain Imaging Study of the 22q13.3 Deletion Syndrome in Childhood. *Pediatrics* **2008**, *122* (2), e376–382. <https://doi.org/10.1542/peds.2007-2584>.
69. Soorya, L.; Kolevzon, A.; Zweifach, J.; Lim, T.; Dobry, Y.; Schwartz, L.; Frank, Y.; Wang, A. T.; Cai, G.; Parkhomenko, E.; Halpern, D.; Grodberg, D.; Angarita, B.; Willner, J. P.; Yang, A.; Canitano, R.; Chaplin, W.; Betancur, C.; Buxbaum, J. D. Prospective Investigation of Autism and Genotype-Phenotype Correlations in 22q13 Deletion Syndrome and SHANK3 Deficiency. *Mol Autism* **2013**, *4* (1), 18. <https://doi.org/10.1186/2040-2392-4-18>.
70. Zwanenburg, R. J.; Ruiter, S. A. J.; van den Heuvel, E. R.; Flapper, B. C. T.; Van Ravenswaaij-Arts, C. M. A. Developmental Phenotype in Phelan-McDermid (22q13.3 Deletion) Syndrome: A Systematic and Prospective Study in 34 Children. *Journal of Neurodevelopmental Disorders* **2016**, *8*. <https://doi.org/10.1186/s11689-016-9150-0>.
71. Hileman, C. M.; Henderson, H. A.; Mundy, P.; Newell, L. C.; Jaime, M. Developmental and Individual Differences on the P1 and N170 ERP Components in Children with and without Autism. *Dev Neuropsychol* **2011**, *36* (2), 214–236. <https://doi.org/10.1080/87565641.2010.549870>.
72. Itier, R. J.; Taylor, M. J. Effects of Repetition and Configural Changes on the Development of Face Recognition Processes. *Dev Sci* **2004**, *7* (4), 469–487. <https://doi.org/10.1111/j.1467-7687.2004.00367.x>.
73. Reese, M. Effects of Age, Gender, and Genotype on Auditory Processing in Phelan-McDermid Syndrome. **2019**.
74. Brittenham, C. Objective Measures of Electrophysiological Responses of Children with Idiopathic Autism Spectrum Disorder and Phelan-McDermid Syndrome to a Contrast-Reversing Checkerboard. *School of Arts & Sciences Theses* **2017**.



75. Siper, P.; George-Jones, J.; Lurie, S.; Rowe, M.; Durkin, A.; Weissman, J.; Meyering, K.; Rouhandeh, A.; Buxbaum, J.; Kolevzon, A. Biomarker Discovery in ASD: Visual Evoked Potentials as a Biomarker of Phelan-McDermid Syndrome. *Biological Psychiatry* **2018**, *83* (9), S9. <https://doi.org/10.1016/j.biopsych.2018.02.040>.
76. Whitehouse, A.; Bishop, D. Do Children with Autism 'Switch off' to Speech Sounds? An Investigation Using Event-Related Potentials. *Developmental science* **2008**, *11*, 516–524. <https://doi.org/10.1111/j.1467-7687.2008.00697.x>
77. Stroganova, T. A.; Kozunov, V. V.; Posikera, I. N.; Galuta, I. A.; Gratchev, V. V.; Orekhova, E. V. Abnormal Pre-Attentive Arousal in Young Children with Autism Spectrum Disorder Contributes to Their Atypical Auditory Behavior: An ERP Study. *PLOS ONE* **2013**, *8* (7), e69100. <https://doi.org/10.1371/journal.pone.0069100>.
78. Madsen, G. F.; Bilenberg, N.; Jepsen, J. R.; Glenthøj, B.; Cantio, C.; Oranje, B. Normal P50 Gating in Children with Autism, Yet Attenuated P50 Amplitude in the Asperger Subcategory. *Autism Research* **2015**, *8* (4), 371–378. <https://doi.org/10.1002/aur.1452>.
79. Isenstein, E.; Durkin, A.; Zhang, Y.; Feldman, E.; Servedio, N.; Harony-nicolas, H.; Buxbaum, J.; Kolevzon, A.; Siper, P.; Foss-Feig, J. Electrophysiological Evidence of Auditory Habituation Abnormalities in Young Adults With Phelan-Mcdermid Syndrome. *Biological Psychiatry* **2018**, *83* (9), S200. <https://doi.org/10.1016/j.biopsych.2018.02.522>.
80. Ponson, L.; Gomot, M.; Blanc, R.; Barthelemy, C.; Roux, S.; Munnich, A.; Romana, S.; Aguilon-Hernandez, N.; Malan, V.; Bonnet-Brilhault, F. 22q13 Deletion Syndrome: Communication Disorder or Autism? Evidence from a Specific Clinical and Neurophysiological Phenotype. *Translational Psychiatry* **2018**, *8* (1), 1–8. <https://doi.org/10.1038/s41398-018-0212-9>.
81. Griskova-Bulanova, I.; Dapšys, K.; Maciulis, V. Does Brain Ability to Synchronize with 40 Hz Auditory Stimulation Change with Age? *Acta neurobiologiae experimentalis* **2013**, *73*, 564–570.
82. Poulsen, C.; Picton, T.; Paus, T. Age-Related Changes in Transient and Oscillatory Brain Responses to Auditory Stimulation during Early Adolescence. *Developmental science* **2009**, *12*, 220–235. <https://doi.org/10.1111/j.1467-7687.2008.00760.x>.
83. Maurizi, M.; Almadori, G.; Paludetti, G.; Ottaviani, F.; Rosignoli, M.; Luciano, R. 40-Hz Steady-State Responses in Newborns and in Children. *Audiology: official organ of the International Society of Audiology* **1990**, *29*, 322–328.
84. Stapells, D.; Herdman, A.; Small, S.; Dimitrijevic, A.; Hatton, J. Current Status of the Auditory Steady-State Responses for Estimating an Infant's Audiogram; 2005; pp 43–59.
85. Engineer, C. T.; Rahebi, K. C.; Borland, M. S.; Buell, E. P.; Im, K. W.; Wilson, L. G.; Sharma, P.; Vanneste, S.; Harony-Nicolas, H.; Buxbaum, J. D.; Kilgard, M. P. Shank3-Deficient Rats Exhibit Degraded Cortical Responses to Sound. *Autism Research* **2018**, *11* (1), 59–68. <https://doi.org/10.1002/aur.1883>.
86. Griskova-Bulanova, I.; Ruksenas, O.; Dapsys, K.; Maciulis, V.; Arnfred, S. M. H. Distraction Task Rather than Focal Attention Modulates Gamma Activity Associated with Auditory Steady-State Responses (ASSRs). *Clinical Neurophysiology* **2011**, *122* (8), 1541–1548. <https://doi.org/10.1016/j.clinph.2011.02.005>.
87. Griskova, I.; Morup, M.; Parnas, J.; Ruksenas, O.; Arnfred, S. M. The Amplitude and Phase Precision of 40 Hz Auditory Steady-State Response Depend on the Level of Arousal. *Exp Brain Res* **2007**, *183* (1), 133–138. <https://doi.org/10.1007/s00221-007-1111-0>.
88. Bensmann, W.; Vahid, A.; Beste, C.; Stock, A.-K. The Intensity of Early Attentional Processing, but Not Conflict Monitoring, Determines the Size of Subliminal Response Conflicts. *Front Hum Neurosci* **2019**, *13*. <https://doi.org/10.3389/fnhum.2019.00053>.
89. Martin, B. A.; Tremblay, K. L.; Korczak, P. Speech Evoked Potentials: From the Laboratory to the Clinic. *Ear Hear* **2008**, *29* (3), 285–313. <https://doi.org/10.1097/AUD.0b013e3181662c0e>.
90. Constantino, J. N.; Davis, S. A.; Todd, R. D.; Schindler, M. K.; Gross, M. M.; Brophy, S. L.; Metzger, L. M.; Shoushtari, C. S.; Splinter, R.; Reich, W. Validation of a Brief Quantitative Measure of Autistic Traits: Comparison of the Social Responsiveness Scale with the Autism Diagnostic Interview-Revised. *J Autism Dev Disord* **2003**, *33* (4), 427–433. <https://doi.org/10.1023/a:1025014929212>.
91. Lord, C.; Rutter, M.; Le Couteur, A. Autism Diagnostic Interview-Revised: A Revised Version of a Diagnostic Interview for Caregivers of Individuals with Possible Pervasive Developmental Disorders. *J Autism Dev Disord* **1994**, *24* (5), 659–685. <https://doi.org/10.1007/BF02172145>.
92. Griskova-Bulanova, I.; Mørup, M.; Parnas, J.; Ruksenas, O.; Arnfred, S. Two Discrete Components of the 20 Hz Steady-State Response Are Distinguished through the Modulation of Activation Level.

*Clinical neurophysiology : official journal of the International Federation of Clinical Neurophysiology* **2009**, *120*, 904–909. <https://doi.org/10.1016/j.clinph.2009.02.175>.

93. Hirano, Y.; Nakamura, I.; Tamura, S.; Onitsuka, T. Long-Term Test-Retest Reliability of Auditory Gamma Oscillations Between Different Clinical EEG Systems. *Front. Psychiatry* **2020**, *11*. <https://doi.org/10.3389/fpsyt.2020.00876>.